REPORT DOCUMENTATION PAGE

AFRL-SR-AR-TR-02-

0373

1. REPORT DATE (DD-MM-YYYY)	2. REPORT TYPE	3. DATES COVERED (From - To)
08/08/2002	Final	01/04/2001 to 31/03/2002

4. TITLE AND SUBTITLE

Instrumentation for Improvement of Gas Imaging Systems

5a. CONTRACT NUMBER

5b. GRANT NUMBER
F49620-01-1-0254

5c. PROGRAM ELEMENT NUMBER

6. AUTHOR(S)

Happer, William

5d. PROJECT NUMBER

5e. TASK NUMBER

5f. WORK UNIT NUMBER

7. PERFORMING ORGANIZATION NAME(S) AND ADDRESS(ES)

Princeton University
Department of Physics
Princeton, NJ 08544

8. PERFORMING ORGANIZATION REPORT NUMBER

9. SPONSORING / MONITORING AGENCY NAME(S) AND ADDRESS(ES)

AFOSR

10. SPONSOR/MONITOR'S ACRONYM(S)

11. SPONSOR/MONITOR'S REPORT NUMBER(S)

12. DISTRIBUTION / AVAILABILITY STATEMENT

Unlimited Distribution

13. SUPPLEMENTARY NOTES

14. ABSTRACT

Funds from the AFOSR:DURIP grant F49620-01-1-0254 have been used to purchase three major pieces of equipment: 1) a nuclear magnetic resonance spectrometer system for studies of the basic physics of hyperpolarized Xe-129 and He-3 gases; 2) a 9.4 T superconducting magnet with a 3 inch room temperature bore; 3) a Verdi diode-pumped Nd:YAG laser to replace the very expensive argon ion laser we have traditionally used for pumping our Ti:sapphire tunable laser. This new equipment has greatly improved the research productivity of our laboratory.

15. SUBJECT TERMS

16. SECURITY CLASSIFICATION OF:			17. LIMITATION OF ABSTRACT	18. NUMBER OF PAGES	19a. NAME OF RESPONSIBLE PERSON
a. REPORT	b. ABSTRACT	c. THIS PAGE			William Happer
U	U	U	UU	11	19b. TELEPHONE NUMBER (include area code) 609-258-4382

FINAL REPORT
For the Research Period
April 1, 2001 through March 31, 2002
for work performed under

Grant AFOSR F49620-01-1-0254

DURIP: INSTRUMENTATION FOR IMPROVEMENT OF GAS IMAGING SYSTEM.

Submitted August 8, 2002
by
William Happer, Principal Investigator

1. Overview

This grant has enabled us to purchase three major pieces of equipment: 1) a nuclear magnetic resonance spectrometer system for studies of the basic physics of hyperpolarized ^{129}Xe and ^{3}He gases; 2) a 9.4 T superconducting magnet with a 3 inch room temperature bore; 3) a Verdi diode-pumped Nd:YAG laser to replace the very expensive argon ion laser we have traditionally used for pumping our Ti:sapphire tunable laser. This new equipment has greatly improved the research productivity of our laboratory.

This equipment supplements our AFOSR-sponsored research on the fundamental physics and applications of spin polarized atoms. One of the most unexpected applications of this work has been in medical imaging of human lungs with laser-polarized ^{3}He and ^{129}Xe gas. Basic research, supported by AFOSR in our group, eventually led to ways to produce liter-atmospheres of ^{3}He and ^{129}Xe gases with spin polarizations of many tens of percent, instead of the parts per million that is normal for magnetic resonance imaging. When inhaled these gases give spectacular images of human lungs, sinuses and other air passages. There is a vigorous clinical center for lung imaging with hyperpolarized gases at the University of Virginia in Charlottesville. That work is sponsored by the international health care company, Nycomed Amersham, which purchased Magnetic Imaging Technologies, Inc., a start up company formed a few years ago to commercialize this AFOSR technology. One of the most interesting gas-imaging activities underway now is a long-term study of the lungs of New York City firemen who survived the collapse of the World Trade Center towers on September 11, 2001.

The work supported by this AFOSR grant has had and will continue to have applications to many technologies of the Unites States Air Force. For example, the Rb clocks used in the GPS satellite system are based on optical pumped gas cells. The basic physical processes operating in these clocks is closely related to that of the cells used to polarize ^{3}He and ^{129}Xe gas for medical imaging. During the research period covered by this report, we accidentally discovered that there are certain novel magnetic resonance transitions, suitable for use in atomic clocks, that are almost unaffected by the spin-exchange broadening that affects the traditional 0-0 clock transition.

2. Disposition of Equipment

30-310 MHz NMR Spectrometer: Using the funds from the grant, we have assembled a rugged, state-of-the art NMR spectrometer, continuously covering the range of frequencies from about 30 MHz to 310 MHz. Combined with the 9.4 Tesla magnet also purchased with funds from this grant, the spectrometer can be used to investigate the magnetic resonance spectra of nuclei ranging from ^{14}N and ^{33}S, with very low magnetic resonance frequencies, to ^{3}He, with a very high frequency. Most importantly, the spectrometer can be used to investigate both magnetic isotopes of xenon,^{129}Xe and ^{131}Xe. Unique features of our apparatus include a high-power amplifier (model 3304C Herley-AMT), with 400 Watts of pulsed power over the entire frequency range and a 9-digit, ultra stable, computer-controlled radio-frequency source (model 310 PTS), with a 16-bit, high-resoultion data acquisition system. The spectrometer is sensitive enough to detect deuterium nuclei in ordinary water. More importantly, it can also detect the nuclear magnetic resonance signals of ^{129}Xe or ^{3}He, at atmospheric pressure and at room temperature. These are the only gases of practical interest for hyperpolarization.

9.4 T Oxford Instruments Magnet: This magnet is an outstanding addition to our experimental capabilities. It has superb homogeneity (10^{-7} over a one inch sphere) and stability (10^{-7} per day). It was installed in record time, only one month after purchase. It is located in a special part of our laboratory from which we exclude magetic tools or other equipment that could be sucked into the magnet and damage it. This new magnet was essential for performing the work described in the attached paper, the first experiment of its kind, and an important contribution to our understanding of spin physics in gaseous media.

Verdi Pump Laser: This solid-state Nd:Yag laser, with diode-laser pumping, has been used to replace an argon-ion laser that is the source of optical pumping light for our Ti:Sapphire laser. The argon-ion laser that it replaced required high-pressure, deionized cooling water from the university chilled water plant. Also the very expensive plasma tubes needed to be replaced every few years. The new Verdi laser needs no external cooling water, since it is much more energy efficient than the argon-ion laser. A closed cycle cooling loop with air cooling is all that is required. We have found the Verdi laser very convenient to use, and we expect to save a great deal of time and money with it in the future. The Verdi laser was used to obtain the data described in the refereed publication and in the attached preprint.

3. Publications

Although the DURIP equipment was only installed last year, it has already made possible new areas of research that we could not have done previously. One refereed paper using this equipment has already been published, and we attach a preprint of one that has just been submitted for review.

D. K. Walter, W. M. Griffith and W. Happer, "Magnetic Slowing Down of Spin Relaxation due to Binary Collisions of Alkali-Metal Atoms with Buffer-Gas Atoms," Phys. Rev. Letters **88** 093004 (2002).

4. Personnel

The following personnel have used the equipment purchased with Grant AFOSR F49620-01-1-0254:

Dr. William Happer, Principal Investigator.

Dr. Nicholas Kuzma, Dicke Fellow and Research Associate.

Dr. Warren Griffith, Research Associate

Dr. Dan Walter, Research Associate, PhD with AFOSR support in 2001.

Mr. Yuan Yu Jau, Graduate Student and PhD candidate.

Ms. Amber Post, Graduate Student and PhD candidate.

High-field measurement of the ^{129}Xe-Rb spin-exchange rate due to binary collisions

Yuan-Yu Jau, Nicholas N. Kuzma, and William Happer
Department of Physics, Princeton University, Princeton, New Jersey 08544
(Dated: July 12, 2002)

We have measured the binary spin-exchange rate coefficient for collisions between Rb and ^{129}Xe atoms at a magnetic field $B = 9.4$ T and in the temperature range $160 < T < 200$°C. The longitudinal spin relaxation rate, $1/T_1$, of ^{129}Xe is dominated by ^{129}Xe-Rb binary collisions. We measured $1/T_1$ with the methods of conventional nuclear magnetic resonance, with no spin enhancement by optical pumping. At the high magnetic field and large gas pressures used in this work, the contribution of ^{129}Xe-Rb molecules to the spin-exchange rate was less than 1% of the binary-collision rate. The Rb atomic number density [Rb] was measured directly from the large Faraday rotation of the polarization of near-resonant light passing through the sample cells. The rate coefficient is $\kappa = d(1/T_1)/d[\mathrm{Rb}] = (1.75 \pm 0.12) \times 10^{-16}$ cm^3/s.

PACS numbers: 32.80.Bx, 33.25.+k, 34.30.+h

I. INTRODUCTION

Spin-exchange optical pumping [1, 2] is becoming a widely-used method to produce large quantities of hyperpolarized ^{3}He [3, 4] and ^{129}Xe [5]. These hyperpolarized gases, where the nuclear spin polarization is much larger than its thermal-equilibrium value, have found applications in magnetic resonance imaging [6–8], neutron spin structure studies [9], surface analysis [10, 11], and experimental tests of fundamental symmetries [12, 13]. Many of these applications would benefit from an increase in spin polarization of the gas. Typical polarizations of ^{129}Xe are still a factor of three lower than those of ^{3}He.

Currently, Rb is most commonly used to transfer angular momentum from the optical-pumping laser light to the nuclei of noble gas atoms. Compared to the spin-exchange processes in the ^{3}He-Rb system [14], where the exchange occurs almost exclusively in binary collisions, spin exchange in ^{129}Xe-Rb [15] has contributions from both binary collisions and from the three-body formation and collisional breakup of ^{129}Xe-Rb van der Waals molecules. A better understanding of the relative importance of binary collisions and van der Waals molecules for polarizing ^{129}Xe will facilitate the design of systems that produce more highly polarized ^{129}Xe. In this paper we describe a new, direct way to measure the binary spin-exchange rate that is free of many of the difficulties that beset earlier measurements.

In their pioneering studies of the ^{129}Xe-Rb system, Volk *et al.* [16] reported a rate coefficient $\kappa = 45 \times 10^{-16}$ cm^3/s. High-permeability shields were used to reduce the magnetic field to less than 10^{-9} T, and the temperature was $T \approx 60$° C. The binary rate coefficient reported by Volk *et al.* is more than a factor of ten larger than that reported in most subsequent work. We mention a few possible reasons for this large discrepancy. The experiments of Volk *et al.* were done with glass cells, containing excess Rb metal and sealed off at room temperature with half a Torr of Xe and N_2 at partial pressures ranging between 10 and 100 Torr. At such low fields and gas pressures, most of the spin relaxation of ^{129}Xe is due to XeRb molecules. It is difficult to extract the relatively small contribution due to binary collisions. The difficulties were compounded by the oversimplified model used to analyze the data. For example, not accounting for the slowing-down of the relaxation due to the angular momentum stored in the nuclear spins of Rb atoms would cause one to substantially underestimate the contribution of XeRb molecules to the relaxation rates.

In subsequent experiments, Cates *et al.* [17] reported a binary rate coefficient of $\kappa = (3.7 \pm 0.7) \times 10^{-16}$ cm^3/s, about 12 times smaller than that of Volk *et al.* The measurements were done at temperatures of about 100° C. The magnetic field was 1.1×10^{-5} T, too small to cause appreciable suppression of the relaxation due to ^{129}Xe-Rb molecules. The model used by Cates *et al.* to analyze their data took into account the nuclear spins of the Rb atoms. To eliminate the effects of ^{129}Xe-Rb molecules, they made measurements in a series of four cells, each containing (at room temperature) about 50 Torr of nitrogen and with xenon pressures ranging from 245 to 1817 Torr. An extrapolation procedure was used to infer the rate coefficient at the infinite pressure limit, where molecular contributions would be negligible. However, recent findings of Kadlecek *et al.* [18], confirmed by work in our laboratory, show that the models of relaxation due to the formation and breakup of loosely bound molecules have serious, and still poorly understood flaws, at gas densities on the order of one amagat or greater. This may have introduced some problems in the pressure extrapolation procedure of Cates *et al.* [17].

The first high-field measurements of rate coefficients were reported by Augustine *et al.* [19, 20]. At a field of B = 2.35 T and a xenon partial pressure of 450 Torr, they reported $\kappa = 2.8 \times 10^{-16}$ cm^3/s. At the same field but at a xenon partial pressure of 1500 Torr, they reported $\kappa = 7.4 \times 10^{-16}$ cm^3/s. It is not clear what might have caused this puzzling dependence on xenon pressure. One would expect a decreasing contribution of XeRb molecules to the relaxation rates with increasing pressure; the increasing three-body formation rate does not compensate for the more rapidly decreasing spin flip

probabilities that result from the shorter molecular lifetimes. At pressures comparable to those used by Augustine *et al.*, but at much smaller magnetic fields, the rate coefficients measured by Cates *et al.* [17] decreased with pressure.

In all three of these early measurements, the number density of Rb atoms [Rb] was not measured directly but was inferred from the measured temperature T of the sample cells. Reference was made to empirically determined formulae for the dependence of [Rb] on T. The Killian [21] formula used by Cates *et al.* [17] gives values for [Rb] that are approximately twice as large as the values given by the Smithells formula [22], used by Volk *et al.* [16] and by Augustine *et al.* [19, 20]. Experience has shown that different cells containing Rb metal at the same temperature can have Rb vapor densities that would differ by factors of two or three from the formulas of Killian or Smithells. The early experiments [16, 17, 19, 20] were done at relatively low [Rb] values, typically [Rb] $< 10^{11}$ cm^{-3}. Contributions of the cell walls [23], magnetic-field gradients, and other mechanisms [24, 25] to the relaxation rates of ^{129}Xe could have affected these earlier measurements.

II. EXPERIMENT

Here we report the first direct measurement of the ^{129}Xe-Rb spin-exchange rate due to binary collisions. We chose high gas pressures ($\gtrsim$ 600 Torr) and a high magnetic field $B = 9.4$ T so that the contribution of RbXe molecules to the spin-exchange rate would be negligible compared to the contribution of binary collisions. We used nuclear magnetic resonance (NMR) to probe the thermal-polarization signal of ^{129}Xe nuclei without optical pumping, and we used the Faraday rotation method [26] to directly determine [Rb]. All measurements were done at high temperatures, between 160° and 200° C, and consequently at much higher Rb densities than in the previous studies [16, 17, 19, 20].

The return of the ^{129}Xe nuclear spin polarization $\langle K_z \rangle$ to its thermal equilibrium value $\langle K_z \rangle_T = \mu_K B/2kT$ (here μ_K is the nuclear magnetic moment of ^{129}Xe and k is the Boltzmann constant) after saturation (destruction) by a train of radio-frequency (rf) pulses is described by

$$\langle K_z \rangle = \langle K_z \rangle_T (1 - e^{-t/T_1}) \ , \qquad (1)$$

where we can write the longitudinal relaxation rate $1/T_1$ of the ^{129}Xe nuclei as

$$\frac{1}{T_1} = [\mathrm{Rb}]\,\kappa + \Gamma' . \qquad (2)$$

In this expression, κ (also denoted as $\langle \sigma_{ex} v \rangle$ in the literature) is the rate coefficient for binary spin-exchange collisions between ^{129}Xe and Rb atoms, and Γ' is the spin-relaxation rate due to other causes, such as contributions from ^{129}Xe-Rb van der Waals molecules [1], wall interactions [23], the formation of Xe_2 molecules [24], or binary Xe-Xe collisions [25]. We will present both theoretical (App. A) and experimental evidence that the values of $1/T_1$ measured in this work are dominated by the binary collision contribution, [Rb] κ.

In our work, we measure the longitudinal ^{129}Xe relaxation rate $1/T_1$ at different cell temperatures T. The main effect of changing the cell temperature is the large, exponential change in Rb density [Rb] $\propto \exp(-T_A/T)$ [the Arrhenius temperature $T_A \approx 9500\,\mathrm{K} \gg T$, so that [Rb] $\propto \exp(T_A \Delta T/T^2) \approx \exp(\Delta T/20\,\mathrm{K})$]. The temperature dependence of the other relaxation rates Γ' is expected to be so small that we take $d\Gamma'/dT = 0$ over the temperature range of our measurements. Our experimental data are consistent with neglecting any temperature variation of Γ'. As we mentioned before, the cell temperature T does not uniquely define [Rb], so at each value of T we independently determined [Rb] by measuring the Faraday rotation of the plane of polarization of a probing laser beam passing through the cell. Our modeling calculations indicate that there should be little change in the binary exchange rate coefficient within the range $160 < T < 200$° C.

The mean binary spin-exchange rate coefficient, κ, is therefore the slope of the experimentally determined plot of $1/T_1$ versus [Rb]. The two quantities, $1/T_1$ and [Rb], must be determined with good experimental accuracy over a range of cell temperatures.

A. Sample Preparation

In this work, we made four spherical alumino-silicate glass cells, 2.5 cm in diameter. These were attached to a glass tube, connected at one end to a gas-handling manifold with pressure monitoring equipment and with cylinders of ultra-pure nitrogen and isotopically enriched xenon (71% ^{129}Xe). The manifold could be evacuated with a turbo-vacuum pump. Attached to the other end of the glass tube was a glass retort with a mixture of RbCl salt and chips of Ca metal. The cells were baked overnight at 400° C under a vacuum of 10^{-7} Torr. Then a gas flame was used to heat the retort and release volatile Rb metal. A few milligrams of rubidium metal were distilled into each of the cells with a gas torch. A cell was then immersed in liquid nitrogen to condense all of the xenon gas of known room-temperature pressure and volume. Nitrogen gas at less than atmospheric pressure (so it could not condense in the cold cell) was added to the manifold and the cell stem was sealed off while the body of the cell remained immersed in liquid nitrogen. With the ideal gas law and the known volume of the cell, it was possible to determine the number densities [Xe] and [N_2], which we quote in units of amagats (1 amg $= 2.69 \times 10^{19}$ cm^{-3}). We prepared cells with four different densities of nitrogen and xenon. After being sealed-off, each cell was put into an oven at 200° C for at least three days in order to make the wall relaxation of ^{129}Xe reach a stable value

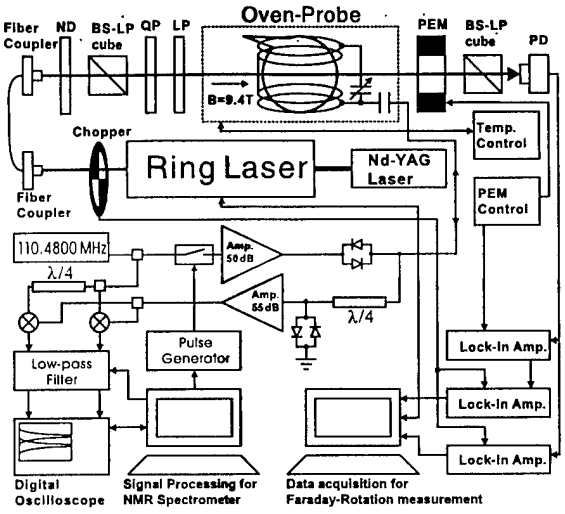

FIG. 1: Schematic diagram of the experimental apparatus built to measure $1/T_1$ and [Rb] for four sealed-off sample cells. More details are given in the text. The rf frequency of the NMR spectrometer was offset from the resonant ^{129}Xe frequency by ~ 1 kHz in order to avoid the low frequency noise background. The wavelength scanning range was from 765 to 795 nm. The oven was ohmically heated up to 200° C.

in the presence of rubidium through a "curing process" [11].

B. NMR Measurement of ^{129}Xe Relaxation Times

Our experimental setup is shown in Fig. 1. The cell and a surrounding NMR coil were mounted inside a heat-insulated, cylindrical oven, suspended in the 89-mm room-temperature bore of a 9.4-T Oxford Instruments superconducting magnet. The inner volume of the oven was heated ohmically using weakly-magnetic high-resistance wire, counter-wrapped 8 cm below the sample cell to avoid distorting the 3×10^{-7} homogeneity of the magnetic field. The temperature was monitored and controlled with two resistive platinum sensors (RTD) and an Omega controller. For the T_1 measurement, a previously described NMR spectrometer [27] was used at a radio frequency set to 110.4800 MHz. The pulse sequence started with a saturating pulse train (100 pulses 500 μs each) that was sent to destroy the thermal polarization of ^{129}Xe. After a variable recovery time τ_r, a single 90° pulse was used to excite a free induction decay (FID) signal. By varying τ_r, we acquired many saturation-recovery curves like the one shown in Fig. 2.

C. Faraday Rotation Measurement of Rb Density

The rubidium atomic number density [Rb] was directly determined by a Faraday rotation measurement. A Ti-sapphire ring laser "Coherent 899-29", pumped by a Nd-YAG "Verdi" laser, was used to generate the probing beam and to scan the wavelength of light. We used a linear polarizer (LP) to ensure that the light entering the cell was linearly polarized.

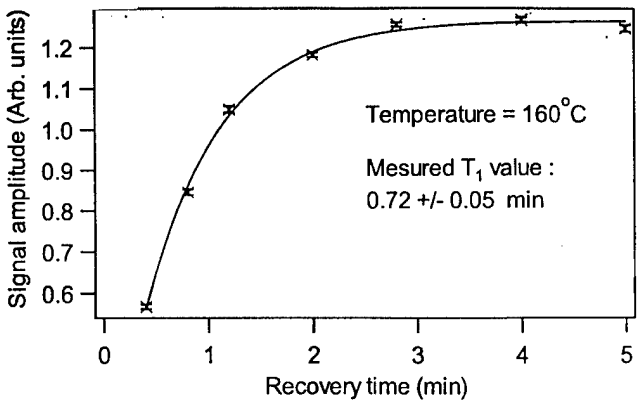

FIG. 2: A representative saturation-recovery measurement of the longitudinal relaxation time T_1 of ^{129}Xe nuclear spins at a given temperature. Details of the NMR procedure are described in the text. Each data point is the average of many FID signals with the same recovery time.

We can describe a light beam in a pure polarization state with two parameters: (i) the orientation angle θ of the semimajor axis of the elliptically polarized light relative to the x axis in a reference plane normal to the beam direction, and (ii) the mean photon spin s, a real number ranging from -1 to $+1$, which describes the relative circular polarization of the light. The ratio a of the minor to the major axis of the ellipse is related to the mean spin s by $a = (1-\sqrt{1-s^2})/s$.

In our experiment, the semimajor axis of the elliptically polarized light entering the cell was oriented at an angle θ_0, which we could vary for experimental convenience. The mean spin s_0 of the light entering the cell was close to zero, since the probe light had nearly perfect linear polarization. Stray birefringence in lenses and windows and reflections from two turning mirrors, not shown in Fig. 1, could change both θ and s, but we verified experimentally that these were negligible effects. The orientation angle of the light emerging from the cell is $\theta = \theta_0 + \Delta\theta$, where the Faraday rotation angle $\Delta\theta$ can be several radians because of large [Rb] and B. In principle, the circular dichroism of the vapor can induce a corresponding change, Δs, in the mean photon spin, but unless the laser wavelength is very close to the center of the absorption lines, Δs will be negligible and the light emerging from the vapor will remain nearly linearly polarized with $s \approx 0$.

To measure the Faraday rotation angle $\Delta\theta$, we set the stress axis of a photo-elastic modulator (PEM) at 45° to the axes of a linearly-polarizing beam-splitter cube (BS-LP) [28]. The angle ψ of the relative phase retardation between the fast and slow axes of the PEM was varied sinusoidally with time t at the frequency $\omega_p/2\pi = 83.4$ kHz. That is, $\psi = \psi_p \sin\omega_p t$, where the

peak phase shift ψ_p is proportional to the driving voltage of the PEM and inversely proportional to the laser wavelength. After passing through the BS-LP, the probe beam was detected with a photodiode, which produced the output voltage,

$$V_{\rm PD} = gI_B(1 + \sqrt{1-s^2}\sin 2\theta\cos\psi + s\sin\psi), \qquad (3)$$

where g is the "gain" of the detection system. The laser power $I_B = I_B(t)$ was mechanically chopped at the frequency $\Omega/2\pi = 153$ Hz.

The laser wavelength λ was scanned with time, and this caused large variations in the angle θ, and also some variation of I_B because of the wavelength dependence of the laser output power. There were also noise fluctuations of I_B.

We can decompose the signal (3) into different frequency harmonics in the familiar way for the frequency modulation, $V_{\rm PD} = V_0 + V_{\omega_p}\sin\omega_p t + V_{2\omega_p}\cos 2\omega_p t + \cdots$, where amplitudes

$$V_0 = gI_B\cdot(1+\sqrt{1-s^2}J_0(\psi_p)\sin 2\theta)\ , \qquad (4)$$

$$V_{\omega_p} = 2gI_B\cdot sJ_1(\psi_p)\ , \qquad (5)$$

$$V_{2\omega_p} = 2gI_B\cdot\sqrt{1-s^2}J_2(\psi_p)\sin 2\theta \qquad (6)$$

are chopped at the relatively low frequency Ω. Here J_n are Bessel functions of the first kind. We empirically adjusted the PEM driving voltage to find the smallest amplitude $\psi_p = \psi_0$ (that is, $\psi_0 = 2.405$) for which $J_0(\psi_p) = 0$. Then $V_0 \doteq gI_B$ became independent of the linear polarization angle θ, and could be used to normalize the signals V_{ω_p} and $V_{2\omega_p}$. A small correction was made to the data to account for the slight variation of $\psi_p \propto 1/\lambda$ over the 1% range of the wavelengths used in this work.

As sketched in Fig. 1, the signal $V_{2\omega_p}$ was detected with two lock-in amplifiers (LIA). The voltage $V_{\rm PD}$ was applied to the first LIA, which was referenced to the PEM drive frequency $2\omega_p$ with a 1 ms integration time. The output of the first LIA was applied to a second LIA, referenced to the probe laser chopping frequency Ω with a 0.1 s integration time. For further analysis, the output voltage of the second LIA is processed with one channel of a digitizing interface (not shown in Fig. 1) to obtain a digitized signal $S_{2\omega_p} \propto V_{2\omega_p}$. This was stored, along with the laser wavelength, in a computer (PC). The signal V_0 was detected by applying $V_{\rm PD}$ to a third LIA, referenced to the chopper frequency Ω and with a 0.1 s integration time, and acquired as described above to obtain the digitized signal $S_0 \propto V_0$. A digitized record of the probe laser wavelength λ was stored along with each pair of values, S_0 and $S_{2\omega_p}$.

For further analysis of the digitized data, we computed the ratio $R = R(\lambda) = S_{2\omega_p}/S_0$. According to (4) and (6) the ratio should be

$$R = S_{2\omega_p}/S_0 = \frac{1}{2}G\sin 2(\theta_0 + \Delta\theta), \qquad (7)$$

where the constant G depends on the different LIA gains in the system. From the well-known theory of Faraday rotation (e. g. see [26]), the rotation angle for the light of wavelength $\lambda = 2\pi c/\omega_\lambda$ close to the strong D_1 and D_2 resonance lines is

$$\Delta\theta = l\,[\mathrm{Rb}]\sum_{Jm\sigma}\frac{A_{Jm\sigma}(\omega_\lambda - \omega_{Jm\sigma})}{[(\omega_\lambda-\omega_{Jm\sigma})^2+\gamma^2/4]}\ , \qquad (8)$$

where l is the optical path length of the laser beam inside the cell and the the quantum numbers $Jm\sigma$ are discussed below. The coefficients $A_{Jm\sigma}$ are

$$A_{Jm\sigma} = \frac{3\pi\,\omega_\lambda r_e c\, f_J\,\sigma\left[C^{J,\,m+\sigma}_{1/2,\,m;\,1,\,\sigma}\right]^2\rho_m}{(2J+1)\,\omega_J}\ , \qquad (9)$$

where $r_e = e^2/m_e c^2 = 2.82\times10^{-13}$ cm is the classical electron radius, e and m_e are the electron charge and mass in cgs units, c is the speed of light, f_J are the oscillator strengths of absorption lines to the $5\,^2\mathrm{P}_J$ excited states. To a good approximation $f_{1/2} = 1/3$ and $f_{3/2} = 2/3$. The resonant frequencies of the two D lines are $\omega_J = 2\pi c/\lambda_J$. These are pressure shifted slightly from the free-atom values of $\lambda_{1/2} = 7947$ Å and $\lambda_{3/2} = 7800$ Å. We assume pressure-broadened Lorentzian lines with the same width at half maximum of γ, as indicated in Eq. (8). The quantity in square brackets is a Clebsch-Gordan coefficient [29]. The index $\sigma = \pm1$ determines whether the absorbed light is left or right circularly polarized. The index $m = \pm1/2$ is the azimuthal electron spin quantum number of the ground state Rb atom, and $\rho_m = Z^{-1}\exp\{-2m\mu_B B/kT\}$ is the probability of a given atom being in a state with the quantum number m. Here $Z = 2\cosh\mu_B B/kT$; the cell temperature is T (in kelvin), and μ_B is the Bohr magneton.

The resonant frequencies $\omega_{Jm\sigma}$ are

$$\omega_{Jm\sigma} = \omega_J + \frac{\mu_B B}{\hbar}[g_J(m+\sigma) - 2m], \qquad (10)$$

where the Zeeman splitting of the excited-state azimuthal levels is determined by the g-values, $g_{1/2} = 2/3$ and $g_{3/2} = 4/3$. Of the eight possible combinations for the summation indeces in Equation (8), $Jm\sigma = (1\pm1/2,\ \pm1/2,\ \pm1)$, the triples $(1/2, 1/2, 1)$ and $(1/2, -1/2, -1)$ are excluded since they refer to non-existent excited-state sublevels with $J = 1/2$ and $m_J = \pm3/2$. So there are only 6 non-zero terms in the sum (8).

From inspection of Eq. (7), we see that the experimentally-determined ratio R on the left can be made equal to the theoretical expression on the right by setting the gain parameter G to twice the maximum value of R, and then fitting the unknown number density [Rb] and the approximately known initial orientation angle θ_0 and the resonance-line wavelengths λ_J.

With the relatively large values of magnetic field (B = 9.4 T) and atomic number densities ([Rb] $\gtrsim$

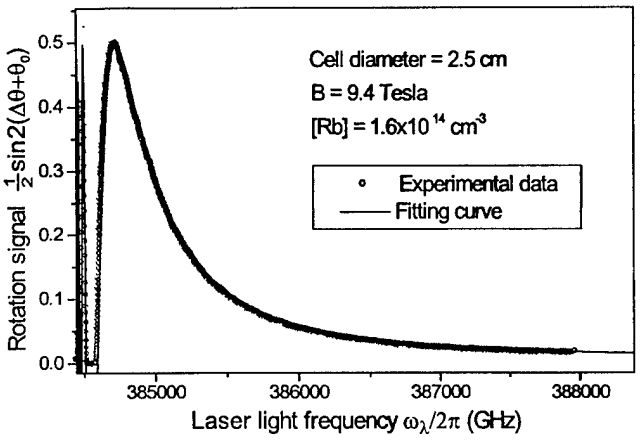

FIG. 3: Experimentally determined Faraday rotation angles $\Delta\theta$ and the best fitting curve, based on (8). Our apparatus did not permit us to record the negative rotation angles that occur at small detunings. The large rotation angle $\Delta\theta$ of the plane of polarization permits an unambiguous fit of the data to the theory, and gives an excellent measurement of the Rb number density [Rb].

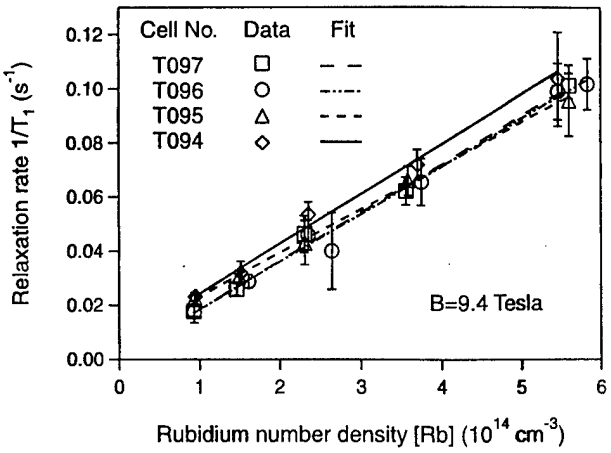

FIG. 4: Measured longitudinal relaxation rates $1/T_1$ plotted versus measured Rb densities [Rb] for the four cells listed in Tab. I. The spin-exchange rate coefficients κ are the slopes of the straight-line fits to the data.

Cell No.	Xe density [amg]	N_2 density [amg]	κ [10^{-16} cm^3/s]
T097	4.0	0	1.78 ± 0.10
T096	0.79	0	1.76 ± 0.16
T095	0.79	1.0	1.60 ± 0.17
T094	0.79	3.0	1.84 ± 0.17

TABLE I: Names, gas content, and experimentally measured values of κ for the four sample cells used in our experiment.

$10^{14}\,\mathrm{cm}^{-3}$) used in our experiments, we could observe several oscillations of the signal $V_{2\omega_p}$, with negligible attenuation, as the laser was tuned toward the resonance line. The resulting highly-structured signal could be fit very precisely (Fig. 3). Our digitizing interface only accepted voltages in the range 0 – 10 V, thus the negative data points are not shown in Fig. 3. To obtain the maximum data with this limitation, the initial orientation angle θ_0 was chosen to make the signal from the second LIA slightly positive in the limit of large positive detunings, $\omega_\lambda - \omega_{3/2} \gg \gamma$. Our data, such as shown in Fig. 3, are much easier to fit than the previous Faraday rotation data [26, 28], taken at much lower values of [Rb] and B, where $\Delta\theta \ll \pi/4$ and thus useful Faraday rotation signals could be observed only for detunings much smaller than the D-line splittings. In present work, we acquired Faraday rotation data with good signal-to-noise ratios for detunings comparable to the D line splittings, so it was necessary to account for both D_1 and D_2 lines in the expression (8), rather than only one, which was appropriate for the earlier work [26, 28] with smaller detunings.

D. Measurement of Stray Circular Polarization

In our experiment, dielectric-coated mirrors are used to change the initial horizontal direction of the laser beam to vertical for propagation up along the bore of the superconducting magnet. Above the magnet, a second mirror was used to change the beam direction back to horizontal to facilitate mounting of the PEM and the light-detection apparatus. To check for any polarization changes produced by the mirrors, we replaced the reference signal at $2\omega_p$ in the first LIA of (Fig. 1) with a reference signal at ω_p. With this arrangement, the output of the second LIA was proportional to V_{ω_p} and thus s, as one can see from Eq. (5). In this way we verified $|s| < 0.07$, so our turning mirrors introduced negligible phase shifts between orthogonal senses of polarization of the probe beam. Other dielectric mirrors, not used in this experiment, introduced quite large phase shifts.

III. RESULTS AND DISCUSSION

Figure 4 is a summary plot of the experimentally measured $1/T_1$ values versus the corresponding values of [Rb], measured with the Faraday rotation technique, for the four cells listed in Tab. I . We fit the data for each cell to a straight line to obtain a slope and an intercept. In accordance with Eq. (2), the slopes are our estimates of κ, while the intercepts are our estimates of the additional relaxation Γ'. Within the experimental error, the four slopes are identical. This experimentally validates our neglecting any temperature dependence of Γ' in the earlier analysis. The values of Γ' extrapolated from the data shown in Fig. 4 are consistent with $\Gamma' = 0$ to within the experimental errors (a direct measurement of Γ' at room temperature gave $\Gamma' = 0.002 \pm 0.001\,\mathrm{s}^{-1}$). The mean slope for the four data sets was $\kappa = (1.75 \pm 0.12) \times 10^{-16}\mathrm{cm}^3/\mathrm{s}$.

We have measured $\kappa(B,T)$ at a magnetic field B = 9.4 T and temperatures T from 433 to 473 K. Based on

the modeling calculations we have done, both with classical path calculations and with the distorted wave Born approximation, we expect the zero-field, 100° C (373 K) value $\kappa(0, 373\,\mathrm{K})$ to be about 20% larger compared to the $\kappa(9.4\,\mathrm{T}, 453\,\mathrm{K})$ value measured here. The 9.4-T magnetic field is sufficient to partially suppress the spin-flip transition probabilities, even for binary collisions, which have durations of only picoseconds. We will report on these modeling calculations in a subsequent paper.

Acknowledgments

This work was supported by the AFOSR grant F49620-98-1-0127 and AFOSR:DURIP grant F49620-01-1-0254. NNK acknowledges R. H. Dicke Fellowship for financial support.

APPENDIX A: HIGH-FIELD CONTRIBUTION OF VAN DER WAALS MOLECULES

For simplicity of notation we assume 100% isotopic abundance of ^{129}Xe. We can write the spin Hamiltonian of a XeRb molecule as

$$H = \hbar\omega S_z + \alpha\,\mathbf{S}\cdot\mathbf{K} = H^{(0)} + H^{(1)}. \qquad \text{(A1)}$$

Here, S is the spin operator of the Rb valence electron, K is the spin operator of the ^{129}Xe nucleus, $\alpha/\hbar \approx 2.0 \times 10^8\ \mathrm{s}^{-1}$ is a representative value of the hyperfine coupling coefficient, averaged over vibrational-rotational states of the molecule, and $\omega = 2\mu_B B/\hbar = 1.65 \times 10^{12}\ \mathrm{s}^{-1}$ is the Larmor frequency of the electron in a magnetic field of 9.4 T. At this large field, we can ignore the nuclear spin of the Rb atom in calculating its spin exchange rates with ^{129}Xe. The zeroth-order part of the Hamiltonian (A1) is $H^{(0)} = \hbar\omega S_z + \alpha S_z K_z$ and the spin-exchange perturbation is $H^{(1)} = \alpha\,(S_+K_- + S_-K_+)/2$.

The ^{129}XeRb molecule will be formed in one of the four spin states $|m_S m_K\rangle$, where $m_S = \pm 1/2$ and $m_K = \pm 1/2$ are the azimuthal quantum numbers of the Rb electron spin and the Xe nuclear spin, correspondingly. These are eigenstates of the zeroth-order Hamiltonian, $H^{(0)}|m_S m_K\rangle = (\hbar\omega m_S + \alpha m_S m_K)|m_S m_K\rangle \approx \hbar\omega m_S|m_S m_K\rangle$. If the molecule is formed in the states $|1/2, 1/2\rangle$ or $|-1/2, -1/2\rangle$ there will be no spin exchange since $H^{(1)}|m_S m_K\rangle = 0$ for these states. The remaining two states, which we denote with $|1\rangle$ for $m_S = 1/2$, $m_K = -1/2$ and $|2\rangle$ for $m_S = -1/2$, $m_K = 1/2$ are coupled, and one can readily verify that $H^{(1)}_{12} = \langle 1|H^{(1)}|2\rangle = \alpha/2$. From first-order perturbation theory, the probability that a molecule, formed in the state $|1\rangle$ at time $t = 0$, will have made a transition to the state $|2\rangle$ at time $t > 0$ is $W = (\alpha/\hbar\omega)^2 \sin^2(\omega t/2)$. Previous experimental work [15, 30] has shown that XeRb molecules are broken up by collisions with other xenon atoms or nitrogen molecules. The mean lifetime τ was found to be very nearly $1/\tau = ([\mathrm{N_2}] + 3.6\,[\mathrm{Xe}]) \times 5.5 \times 10^9\ \mathrm{s}^{-1}\ \mathrm{amg}^{-1}$. A Xe atom is approximately 3.6 times as likely to break up a XeRb molecule as an N_2 molecule. For cell T094 we find $\tau = 31$ ps. Therefore $\tau\omega = 51$. The magnetic field is large enough that the probability of a spin flip from state $|1\rangle$ to $|2\rangle$ is independent of the molecular lifetime τ and is $\langle W\rangle = (\alpha/\hbar\omega)^2/2 = 7.3 \times 10^{-9}$. The factor of $1/2$ is from the mean value of $\sin^2(\omega t/2)$.

A XeRb molecule can form in simultaneous collisions of a Xe atom, a Rb atom and a third atom or molecule. The third body is another Xe atom or a nitrogen molecule N_2 in our cells. The number density of molecules will therefore grow at the rate

$$\frac{d}{dt}[\mathrm{XeRb}] = \zeta\,[\mathrm{Xe}][\mathrm{Rb}]. \qquad \text{(A2)}$$

where $\zeta = Z_\tau\,([\mathrm{N_2}] + 3.6\,[\mathrm{Xe}]\,)$. Three-body rate coefficients Z_τ have been determined from previous experimental work. For nitrogen [15], $Z_\tau = 3.9 \times 10^{-32}\ \mathrm{cm}^6/\mathrm{s}$ (after rescaling the original data by the ratio of temperatures 349 K/453 K). For cell T094 this implies that $\zeta = 6.2 \times 10^{-12}\ \mathrm{cm}^3/\mathrm{s}$. Denoting the number densities of spin-up and spin-down atoms with the supscripts + and − respectively, we see the the formation of XeRb molecules will cause $[\mathrm{Xe_+}]$ to change at the rate

$$\frac{d}{dt}[\mathrm{Xe_+}] = \zeta\,([\mathrm{Xe_-}][\mathrm{Rb_+}] - [\mathrm{Xe_+}][\mathrm{Rb_-}])\langle W\rangle. \qquad \text{(A3)}$$

We have neglected the slight difference in the forward and reverse rates, an effect we will analyze in the next appendix. In keeping with this approximation we have neglected the thermal polarization of the Rb atoms. Setting $[\mathrm{Rb_\pm}] = [\mathrm{Rb}]/2$, and $[\mathrm{Xe_\pm}] = [\mathrm{Xe}](1/2 \pm \langle K_z\rangle)$ in (A3) we find

$$\frac{d}{dt}\langle K_z\rangle = -\kappa'\,[\mathrm{Rb}]\langle K_z\rangle, \qquad \text{(A4)}$$

where the three-body rate coefficient for cell T094 is

$$\kappa' = \zeta\,\langle W\rangle = 4.5 \times 10^{-20}\mathrm{cm}^3/\mathrm{s}. \qquad \text{(A5)}$$

This is 3900 times smaller than the experimental result, $\kappa = 1.75 \times 10^{-16}\ \mathrm{cm}^3/\mathrm{s}$. Similarly small estimates are found for the other cells. We conclude that XeRb molecules cannot contribute more than 0.1% to the rates measured in these experiments. The estimated XeRb contribution is substantially smaller than the experimental error. The uncertainties in the estimates of the molecular formation and breakup rates are not large enough to change this conclusion. Furthermore, our experimentally measured rate coefficients have no systematic dependence on the gas pressure of the cells, and are the same to within the experimental error. This is to be expected if the rates are due to binary collisions, but not if the rates include a substantial contribution from the formation and breakup of XeRb molecules.

APPENDIX B: FORWARD AND REVERSE RATES

Here we discuss the meaning of "the binary rate coefficient" κ, which was measured in these experiments. A spin-flip binary collision where the electron spin flips up while the nuclear spin flips down is endothermic by the sum of the electron and nuclear spin flip energies,

$$\Delta E = \hbar\omega + 2\mu_K B. \tag{B1}$$

The magnetic moment of the ^{129}Xe nucleus is μ_K. We denote the rate coefficient for such endothermic collisions by κ_{12}. The inverse collision, in which the electron flips down while the nucleus flips up, is exothermic by ΔE. We will denote exothermic rate coefficient by κ_{21}. Detailed balance requires that these two rates differ by a Boltzmann factor. They can therefore be written as

$$\kappa_{21} = \kappa e^{\Delta E/2kT}, \quad \text{and} \quad \kappa_{12} = \kappa e^{-\Delta E/2kT}. \tag{B2}$$

where

$$\kappa = \sqrt{\kappa_{12}\kappa_{21}}. \tag{B3}$$

For binary collisions, the rate equation analogous to (A3) is

$$\frac{d}{dt}[\mathrm{Xe}_+] = \kappa_{12}[\mathrm{Xe}_-][\mathrm{Rb}_+] - \kappa_{21}[\mathrm{Xe}_+][\mathrm{Rb}_-]. \tag{B4}$$

Inserting $[\mathrm{Rb}_\pm] = [\mathrm{Rb}](1/2 \pm \langle S_z\rangle)$ and $[\mathrm{Xe}_\pm] = [\mathrm{Xe}](1/2 \pm \langle K_z\rangle)$ for the number densities of spin-up and spin-down atoms into (B4) we find

$$\begin{aligned}\frac{d}{dt}\langle K_z\rangle &= [\mathrm{Rb}]\kappa_{21}(1/2 - \langle K_z\rangle)(1/2 + \langle S_z\rangle) \\ &- [\mathrm{Rb}]\kappa_{12}(1/2 + \langle K_z\rangle)(1/2 - \langle S_z\rangle).\end{aligned} \tag{B5}$$

We assume the transition rate between the two electron spin states of the Rb atom due to spin exchange with the nuclei of ^{129}Xe atoms is much slower than the transition rate due to spin-rotation collisions, diffusion to the cell walls, and other relaxation mechanisms independent of the nuclear spin polarization of the ^{129}Xe. Then we can take the electron spin polariation in (B5) to be time-independent and equal to the thermal-equilibrium value,

$$\langle S_z\rangle_T = (1/2)\tanh(\hbar\omega/2kT). \tag{B6}$$

Substituting (B6), (B2), and (B1) into (B5) we find

$$\frac{d}{dt}\langle K_z\rangle = \frac{1}{T_1}\left(\langle K_z\rangle_T - \langle K_z\rangle\right), \tag{B7}$$

where $\langle K_z\rangle_T = (1/2)\tanh(\mu_K B/kT) \approx \mu_K B/2kT$. The solution of (B7) is Eq. (1). The longitudinal relaxation rate is

$$\frac{1}{T_1} = \frac{\cosh(\mu_K B/kT)}{\cosh(\hbar\omega/2kT)}[\mathrm{Rb}]\kappa = 0.9996\,[\mathrm{Rb}]\,\kappa. \tag{B8}$$

The ratio of the cosh functions is 0.9996 for $B = 9.4$ T and $T = 450$ K, the mean temperature of our experiments. So the measured slope of $1/T_1$ versus [Rb] gives κ, the mean of the endothermic and exothermic rate coefficients, to better than one part per thousand.

[1] S. Appelt *et al.*, Phys. Rev. A **58**, 1412 (1998).
[2] T. G. Walker and W. Happer, Rev. Mod. Phys. **69**, 629 (1998).
[3] T. E. Chupp, M. E. Wagshul, K. P. Coulter, **A**. B. McDonald, and W. Happer, Phys. Rev. C **36**, 2244 (1987).
[4] J. R. Johnson *et al.*, Nucl. Instrum. Methods Phys. Res. A **356**, 148 (1995).
[5] B. Driehuys, G. D. Cates, E. Miron, K. Sauer, **D**. K. Walter, and W. Happer, Appl. Phys. Lett. **69**, 1668 (1996).
[6] M. S. Albert *et al.*, Nature **370**, 199 (1994).
[7] H. Middleton *et al.*, Magnet. Reson. Med. **33**, 271 (1995).
[8] J. R. MacFall *et al.*, Radiology **200**, 553 (1996).
[9] P. L. Anthony *et al.*, Phys. Rev. Lett. **71**, 959 (1993).
[10] D. Raftery, H. Long, T. Meersmann, P. J. Grandinetti, L. Reven, and A. Pines, Phys. Rev. Lett. **66**, 584 (1991).
[11] Z. Wu, W. Happer, M. Kitano, and J. Daniels, Phys. Rev. A **42**, 2774 (1990).
[12] N. R. Newbury *et al.*, Phys. Rev. Lett. **67**, 3219 (1991).
[13] M. V. Romalis and M. P. Ledbetter, Phys. Rev. Lett. **87**, 067601 (2001).
[14] A. B. A. Baranga, S. Appelt, M. V. Romalis, C. J. Erickson, A. R. Young, G. Cates, and W. Happer, Phys. Rev. Lett. **80**, 2801 (1998).
[15] X. Zeng, Z. Wu, T. Call, E. Miron, D. Schreiber, and W. Happer, Phys. Rev. A **31**, 260 (1985).
[16] C. H. Volk, T. M. Kwon, and J. G. Mark, Phys. Rev. A **21**, 1549 (1980).
[17] G. D. Cates *et al.*, Phys. Rev. A **45**, 4631 (1992).
[18] S. Kadlecek, L. W. Anderson, and T. G. Walker, Phys. Rev. Lett. **80**, 5512 (1998).
[19] M. P. Augustine and K. W. Zilm, Chem. Phys. Lett. **280**, 24 (1997).
[20] M. P. Augustine and K. W. Zilm, Mol. Phys. **89**, 737 (1996).
[21] T. Killian, Phys. Rev. **27**, 578 (1926).
[22] C. J. Smithells, *Metals Reference Book* (Butterworths, London, 1962), vol. 2, p. 655.
[23] X. Zeng, E. Miron, W. A. VanWijngaarden, D. Schreiber,

and W. Happer, Phys. Lett. A **96**, 191 (1983).
[24] B. Chann, I. A. Nelson, L. W. Anderson, B. Driehuys, and T. G. Walker, Phys. Rev. Lett. **88**, 113201 (2002).
[25] I. L. Moudrakovski *et al.*, J. Chem. Phys. **114**, 2173 (2001).
[26] Z. Wu, M. Kitano, W. Happer, M. Hou, and J. Daniels, Appl. Optics. **25**, 4483 (1986).
[27] B. Patton, N. N. Kuzma, and W. Happer, Phys. Rev. B **65**, 020404 (2002).
[28] C. J. Erickson, Ph.D. thesis, Princeton University (2000).
[29] D. A. Varshalovich, A. N. Moskalev, and V. K. Khersonskii, *Quantum Theory of Angular Momentum* (World Scientific, Singapore, 1988).
[30] M. A. Bouchiat, J. Brossel, and L. C. Pottier, J. Chem. Phys. **56**, 3703 (1972).